Fabrication of gecko foot-hair like nano structures and adhesion to random rough surfaces*

Domenico Campolo, Steven Jones and Ronald S. Fearing
Department of EECS, University of California, Berkeley, CA 94720

***Abstract*— In this work the effect of substrate roughness on the adhesion of gecko foot-hair like nano structures as opposed to solid elastic materials is described and models of both synthetic nano-hairs and hair-substrate interaction are developed. First, by combining linear beam theory and geometric constraints, a nonlinear elastic model for the hair is derived. Then it is shown how for a given random surface, once its Zero Order Hold (ZOH) model is acquired through Atomic Force Microscopy, only the height distribution is needed to compute pull-off forces.**

In the effort of replicating gecko foot-hair adhesive properties, we synthesized arrays of nano hairs by casting polyurethane into a nano-pore array. Hairs of controlled size, in the range of 20-60 microns long and 200 nanometers thick, were thus fabricated, imaged via Scanning Electron Microscope (SEM).

Elastic properties of polyurethane are measured and then fed into a model, based on cantilever beam theory, which, together with the height distribution of sample surfaces, provides a prediction for pull-off forces as well as a description of the hysteresis phenomena arising in push-in/pull-off cycles.

I. Introduction

Geckos' ability of climbing surfaces, whether wet or dry, smooth or rough, has attracted scientists attention for decades. By means of dry and compliant micro/nano-scale high aspect ratio beta-keratin structures at their feet, geckos manage to adhere to almost any surface with a controlled contact area [1]. It has been shown that adhesion is mainly due to molecular forces such as van der Waals force [2]. In the effort of replicating the dry adhesive properties [3] of gecko foot-hair, in this paper the adhesion between nano-hair like elastic structures and random rough surfaces is described.

Despite its compliance, a solid material fails to perfectly conform to a very rough substrate when the elastic energy required to fill out a cavity of the substrate exceeds the thermodynamic energy gained from the contact itself [6]. The elastic energy at a point $\mathbf{x}$ depends on the deformation at the point itself, determined by $s(\mathbf{x})$, as well as the deformation occurring at nearby points which can be determined by the spatial derivatives of $s(\mathbf{x})$, evaluated at $\mathbf{x}$, via the Taylor series expansion. For a qualitative result, see [6]. If η and λ represent respectively perpendicular and parallel roughness length scales (for a purely sinusoidal substrate, λ would be the spatial period and η the amplitude as in [5]), the elastic energy required to fill out a cavity can be estimated to be $U_{el} \approx E\lambda\eta^2$ where E is the Young's modulus of the elastic material[1].

Since the elastic deformation is confined in a volume of the order of λ^3, the *density* of elastic energy would be $\mathcal{U}_{el} \approx E\,\eta^2/\lambda^2$. The adhesion energy density, instead, is $\mathcal{U}_{ad} \approx -\Delta\gamma$, where $-\Delta\gamma$ is the change of surface free energy upon contact.

For rough surfaces $\lambda \ll \eta$. The balance $\mathcal{U}_{ad} - \mathcal{U}_{el}$ becomes negative, i.e. elastic energy works against adhesion, making elastic solid materials such as rubber not suitable for adhesive purposes.

On the other hand, when hair-like elastic surfaces are considered, deformation of a single hair is not affected by the deformation of neighbor hairs. In other terms, elastic energy at a point $\mathbf{x}$ only depends on $s(\mathbf{x})$ and not on its spatial derivatives for static contact.

This point, pictorially sketched in Fig.(1), will be developed in detail in the next section.

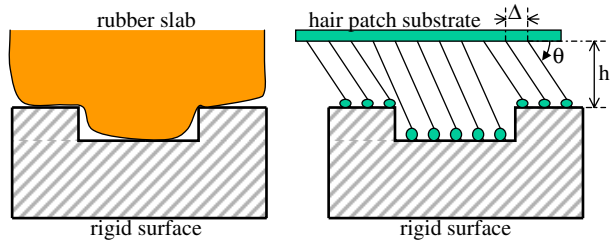

Fig. 1. Partial contact in the case of a solid elastic materials (left) and a hair-like one (right).

II. Hair-surface interaction model

In this section, first a simple model for a single hair will be developed and then the interaction of a hair patch with a randomly rough surface will be modelled.

A. Single hair model: nonlinear stiffness and hysteresis

A hair patch, as the one depicted on the right side of Fig.(1), consists of an array of similar hairs whose base is fixed onto a substrate (at an angle θ_0) and whose tip will be mainly responsible for contacting a randomly rough surface. In order to evaluate the compliance of a single hair, a cantilevered beam model will be deployed. Although gecko foot hairs exhibit a

*This work was supported by DARPA N66001-00-C-8047 and N66001-01-C-8072.

[1]As in [6], consider a cavity of planar dimension λ^2 and depth η. $U_{el} = E\epsilon^2\,Vol$, where ϵ is the strain and Vol is the volume containing the deformation. Such a deformation is assumed to be confined in cube $Vol = \lambda^3$ and thus strain can be estimaded as $\epsilon = \eta/\lambda$ which leads to $U_{el} \approx E\lambda\eta^2$.

curvature throughout their length, our synthetic hairs will be straight due to fabrication constraints. Nevertheless, with slight modifications, the model can be extended to real gecko hairs by considering initially curved cantilever beams.

Consider a cantilevered circular beam of radius $r = 100nm$ and length $l = 60\mu m$ made out of polyurethane, whose Young's modulus was experimentally estimated to be $E \approx 1GPa$. Such a cantilever will prove to be very stiff when subjected to axial tension/compression but very compliant with respect to lateral (transversal) bending. In fact, from basic beam theory, the axial stiffness k_a (axial force to axial displacement ratio) and the transversal stiffness k_θ (shear force to tip lateral displacement ratio) are:

$$\begin{array}{rcl} k_a & = & \frac{\pi r^2 E}{l} \\ k_\theta & = & \frac{3\pi r^4 E}{4l^3} \end{array} \quad (1)$$

Thus $k_\theta / k_a \approx r^2/l^2$, i.e. $k_\theta \ll k_a$. Thus, each hair is equivalent to a rigid link ($k_a \rightarrow \infty$) which is free to rotate about its base joint. The transversal stiffness of the beam is taken into account by an equivalent torsional stiffness k_{rot}. The torsional stiffness relates torques (transversal forces times hair length l) to angular displacement (tip transversal displacement divided by hair length l) and therefore $k_{rot} = k_\theta \ l^2$.

When contacting locally flat surfaces[2], adhesion will constrain the hair tip to lie on the surface (as long as a single hair adhesion force $F_0 \approx 200nN$ is not exceeded). Pull-off forces can be experimentally characterized by letting the hair patch undergo vertical, i.e. normal to the surface, cyclic displacements. Similarly, each hair base will be thought as constrained, at any time, to the same vertical displacement. A convenient quantity is the projection of the hair length onto the vertical, i.e. normal to the surface, z-axis $h = l \sin(\theta)$. For a given h (around the rest value $h_0 = l \sin(\theta_0)$) there exists a unique angle θ such that the tip makes contact while preserving the hair length.

Given the height h of the hair patch with respect to the surface, the corresponding angle $\sin(\theta) = h/l$ can be determined and therefore the corresponding torsional torque $-k_{rot}(\theta - \theta_0)$. For a frictionless surface, the tip is subject to a total force $F_0 - F_n$, where $F_0 \approx 200nN$ is the adhesion force and $F_n \geq 0$, in the opposite direction, is the normal[3] surface reaction, resulting in a zero total moment:

$$(F_0 - F_n)\, l \cos(\theta + \Psi) = k_{rot}(\theta - \theta_0) \quad (2)$$

where Ψ is the tilting angle between the hair patch substrate and the (locally) flat surface, as in Fig.(2). In order to keep the model simple the assumption $\Psi \rightarrow 0$ will be made throughout the paper[4]. In case of friction, by letting the hair patch freely move laterally in reaction to forces parallel the surface, the same result can still be obtained.

[2]Although randomly rough, many surfaces of interest can be considered flat at a length scale of the order of the hair thickness.

[3]Because of the frictionless assumption.

[4]This is the strongest assumption so far. In many cases Ψ can be considered small but in general it can be said that the average Ψ is zero over the whole surface and that also its effect will cancel out.

The hair elastic behavior can be summarized as:

$$\left\{ \begin{array}{rcl} h & = & l \sin(\theta) \\ F & = & l^{-1} \, k_{rot} \, \frac{\theta - \theta_0}{\cos(\theta)} \end{array} \right. \quad (3)$$

where $F = F_0 - F_n \leq F_0$ is the force exerted at the base of the hair (at the patch substrate).

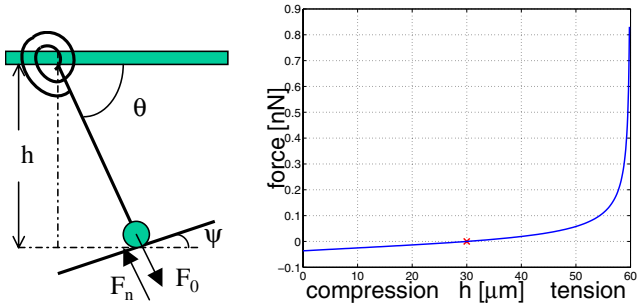

Fig. 2. Left: hair model consisting of a rigid link with torsional stiffness k_{rot}. Right: force $F = F_0 - F_n$ to distance h for a single hair. The cross ($\times$) denotes the rest position $h_0 = l \sin(\theta_0) = l/2$ for $\theta_0 = \pi/6$.

For a single hair, the force F vs. displacement h, as in Eq.(3), is shown in Fig.(2). Clearly, the hair is very compliant around the rest position h_0 while it becomes very stiff as $\theta \rightarrow \pi/6$, i.e. $h \rightarrow l$.

At pull-off, $F_n = 0$ and $\theta = \theta_{max}$, i.e. the hair will reach its maximum bending but contact will be broken slightly before the hair is perfectly vertical ($\pi/2$).

This allows evaluating the maximum stretching of the hair as:

$$\delta_{max} \triangleq h_{max} - h_0 = l\,[sin(\theta_{max}) - sin(\theta_0)] \quad (4)$$

Such a simple system, i.e. a spring with an adhesive tip, contains the basic elements to show hysteresis in a push-in/pull-off cycle as sketched in Fig.(3)

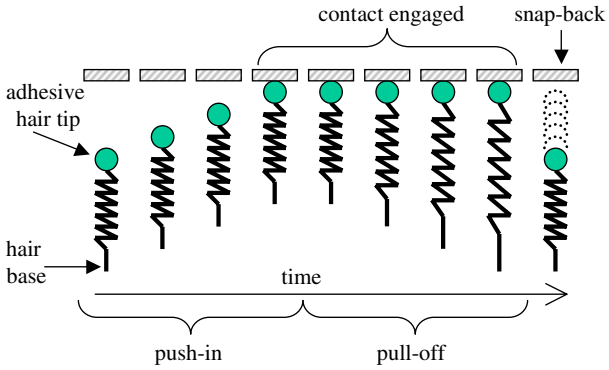

Fig. 3. Push-in / pull-off cycle for a single hair (the same hair is represented at different times). Hysteresis appears when considering the amount of spring elongation (proportional to the elastic force) versus spring base (i.e. the hair patch base) displacement.

B. Roughness of surface

Consider a hair patch facing a randomly rough surface such as the one in Fig.(4). Every hair will face a different point $\mathbf{x}$

on the surface, let $s(\mathbf{x})$ be the surface height at $\mathbf{x}$. For any two points $\mathbf{x_1}$ and $\mathbf{x_2}$ of same height, i.e. $s(\mathbf{x_1}) = s(\mathbf{x_2})$, the hair will undergo the same deformation according to Eq.(3), at anytime. Hairs facing the same surface level can thus be considered equivalent and the pull-off forces of a class of equivalent hairs are simply given by the pull-off forces generated by a single hair times the number of hairs in that particular class.

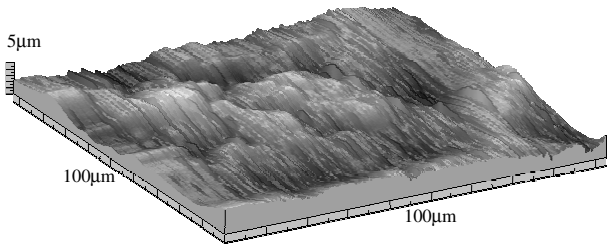

Fig. 4. Atomic Force Microscope (AFM) image of a sample surface.

Previous arguments allow one to reduce the two-dimensional problem of a surface to simply determining a one-dimensional height distribution. Referring to Fig.(4), instead of considering $0 \leq s(\mathbf{x}) \leq 5.3\mu m$ for any $\mathbf{x}$ in a $100\mu m \times 100\mu m$ patch, the percentage of area (or equivalently the percentage of hairs facing an area) whose height lies within given ranges can be determined. In Fig.(5) the whole height distribution was divided into 20 intervals and, for example, about 12% of the whole area is at a height between $2.25\mu m$ and $2.50\mu m$.

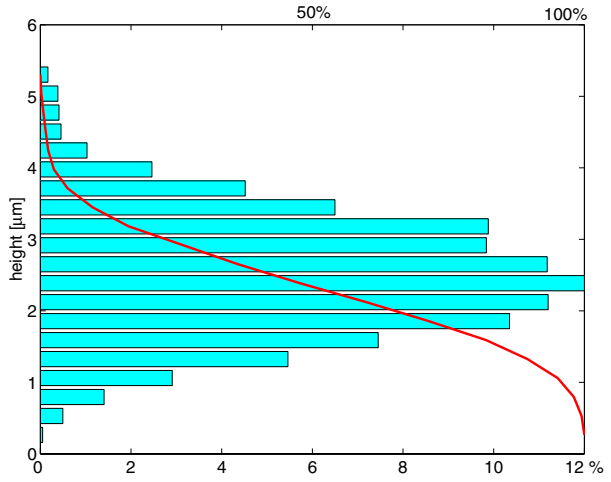

Fig. 5. Abbot-Firestone plots of a sample surface. The histogram represents percentage of surface area (readings at the bottom horizontal axis) at a given depth (vertical axis). The solid curve represents percentage of surface area (readings at the top horizontal axis) above a certain depth (vertical axis).

C. Hair-surface interaction

In Fig.(5) only 20 intervals were used for sake of clarity but, in order to simulate the overall hair patch interaction with the surface in Fig.(4), $N = 256$ equally spaced intervals $I_i = [s_{i-1}\ s_i]$, where $s_{i-1} < s_i$, $0\mu m = s_0$, and $s_N = 5.3\mu m$, will be used. The surface will now be supposed to assume only discrete values s_i.

Consider a system of coordinates where the z-axis is normal to the (mean) surface and points towards the hair patch. Set the origin at the surface absolute minimum. Let every hair base be at $z = z_b$, for an undeformed hair the tip would be at $z_0 = z_b - h_0$, where $h_0 = l\, sin(\theta_0)$ as before.

Consider a situation where the patch is close enough to the surface so that $z_0 = s_j$ for some j. Clearly, every hair facing s_i with $i > j$ will be in compression. A priori, nothing can be said for hairs facing s_i with $i < j$ since it depends on the history of hairs; some hairs might in fact be stretching out reaching depths below the level z_0.

Let's consider an initial situation where no contact is made, i.e. the hair patch is very far from the surface. Then the hair patch is (slowly) lowered until some hairs start making contact, i.e. $z_0 = s_N$. If z_0 is monotonically decreased down to a certain level, say $z_0 = s_{j_1}$, contact will be made for $i > j_1$ but not for $i < j_1$.

If z_0 is now brought to a *slightly* higher level, say s_{j_0} with $j_0 > j_1$ then all the hairs facing s_i such that $j_0 < i < j_1$ will be in a stretching condition. *Slightly* here means that maximum stretching δ_{max} should not be exceeded.

Hairs contacting the level s_{j_1} will be subject to the highest amount of stretching. If we keep increasing z_0, hairs in contact with s_{j1} will reach maximum stretching δ_{max}, and eventually break contact, exactly when $z_0 - s_{j_1} = \delta_{max}$.

The previous example argues that there exists a level z_1 such that $z_0 - \delta_{max} \leq z_1 \leq z_0$ and that for a level s_i:

if	$s_i > z_0$	: hairs are in contact (compression)
if	$z_1 < s_i < z_0$	: hairs are in contact (tension)
if	$s_i < z_1$	: no contact is made

As for the dynamics of z_1, as z_0 slowly varies in discrete time t_n, starting from the initial condition $z_1 = z_0$ the following is easily derived:

if @ t_{n-1}			$then$ @ t_n
$z_1 = z_0$	and	$\dot{z}_0 < 0$	$z_1 = z_0$
$z_1 = z_0 - \delta_{max}$	and	$\dot{z}_0 > 0$	$z_1 = z_0 - \delta_{max}$
$otherwise$			$z_1 = const.$

(5)

where $\dot{z}_0$ is the time derivative of z_0 and $z_1 = const$ means that $z_1(t_n) = z_1(t_{n-1})$.

At any time t_n and at any height s_i such that $s_i \geq z_1$, contact is made. The force F_i of a single hair making contact with s_i can be found by Eq.(3) where $h = h_0 + z_0 - s_i$.

The number of hairs (per unit area) n_i in contact with s_i can be derived by the height distribution, as in Fig.(5).

The total pressure, at any time, can be computed as:

$$P_{tot} = \sum_{i=i_1}^{N} n_i\, F_i \tag{6}$$

where i_1 is the index for which $s_{i_1} = z_1$.

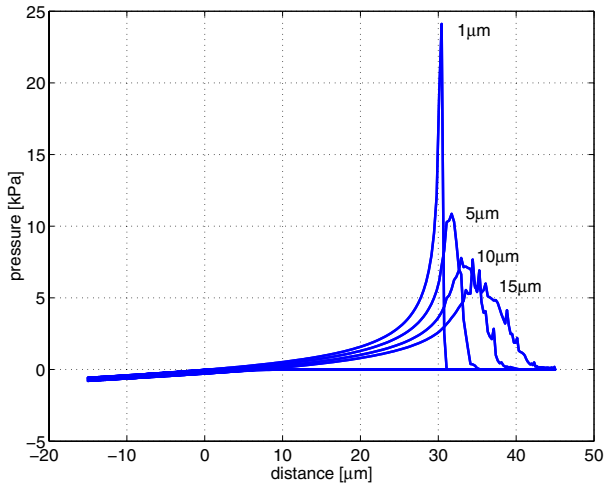

Fig. 6. Simulated push-in/pull-off cycle. Adhesive pressure is plotted versus z_0 (related to the distance between hair patch and minimum surface level) for surface roughness of $1\mu m$, $5\mu m$, $10\mu m$, and $15\mu m$. For each curve a large amout of hysteresis arises (the bottom flat part is common to all curves).

Simulation results, shown in Fig.(6), of adhesive pressure versus z_0 for push-in/pull-off cycles reveal, as expected, a large amount of hysteresis. MATLAB was used to implement the method previously described. Polyurethane cylindrical hairs, $60\mu m$ long, with $100nm$ radius, with $200nN$ adhesive force at the tip, forming a $\pi/6$ angle with the surface have been modelled. The AFM image shown in Fig.(4) was used as a random $5\mu m$ rough test surface. By re-scaling, the other $1\mu m$, $10\mu m$, and $15\mu m$ rough surfaces were also obtained.

Clearly, Fig.(6) shows how roughness influences adhesion and in particular allows, for a given roughness, to estimate pull-off forces, i.e. maxima of the curves. Although data for a specific surface were used, results are quite general. Similar results can be found in [7], although hysteresis is not mentioned, where a Gaussian height distribution was assumed and elastic energy was considered instead of elastic forces.

Different surfaces can thus be considered equivalent when their height distribution is similar enough since that is all that is needed for computing pull-off forces. A statistical knowledge of height distribution will also allow estimating adhesion for a given hair-like nanostructure.

III. Fabrication of nano hairs

Synthetic hair fabrication begins with a negative mold. Alumina oxide self-assembly nanopore membrane (Anodisc, Whatman Inc.) with pores of $0.2\mu m$ diameter, $60\mu m$ length, and $10^9/cm^2$ pore density is placed on an adhesive surface (Gel-Pak 8x, Gel-Pak Inc.) to create a seal on one end of the alumina membrane pores.

Evacuation of the membrane pores occurs as the sample is brought under vacuum, and liquid polyurethane (TC-882, BJB Enterprises) is applied to the exposed membrane surface.

The sample is then returned to atmospheric pressure; membrane pores remain under vacuum due to adhesive material and polyurethane seals. This pressure gradient is relieved as atmospheric pressure presses liquid polyurethane into the evacuated pores, and the assembly is allowed to cure.

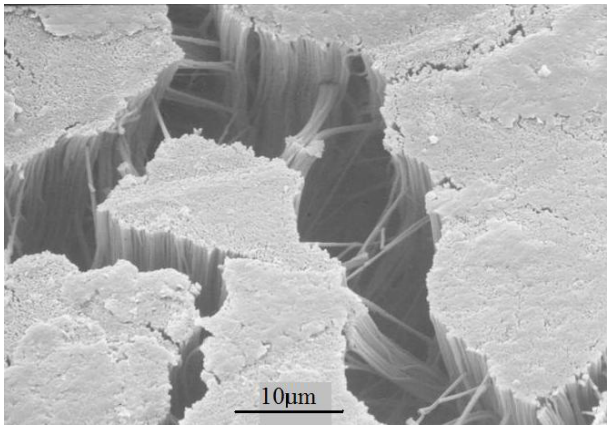

Fig. 7. Scanning electron microscope (SEM) image of synthetic $60\mu m$ long polyurethane hairs.

Desired hair morphology is realized through a micro-polishing process, which allows variation in hair length, sample planarity, and hair-tip roughness. NaOH selectively etches the alumina oxide membrane from around the cured polyurethane, and hair-like polyurethane structures remain. A final cleaning step occurs in a sonic water bath to remove remnant alumina oxide and hair debris. Fig.(7) depicts an SEM of a $1.33cm^2$ patch of hairs created with these methods.

References

[1] K. Autumn, et al., *Adhesive force of a single gecko foot-hair*, Nature, vol. 405, pp. 681-685, 2000.

[2] K. Autumn, et al., *Evidence for van der Waals attachment by Gecko foot-hair inspires design of synthetic adhesive*, Proc. of the National Academy of Science, 2002.

[3] M. Sitti and R.S. Fearing, *Synthetic Gecko Foot-Hair Micro/Nano-Structures as Dry Adhesives,* to appear, Journal of Adhesion Science and Technology, 2003.

[4] B.N.J. Persson, *Adhesion between an elastic body and a randomly rough hard surface*, The European Physical Journal E, vol. 8, pp 385-401, 2002.

[5] B.N.J. Persson, *The effect of surface roughness on the adhesion of elastic solids*, Journal of Chemical Physics, vol. 115, n. 12, pp 5597-5610, 2001.

[6] B.N.J. Persson, *Theory of rubber friction and contact mechanics*, Journal of Chemical Physics, vol. 115, n. 8, pp 3840-3861, 2001.

[7] B.N.J. Persson, *On the mechanism of adhesion in biological systems*, Journal of Chemical Physics, vol. 118, n. 16, pp 7614-7620, 2003.